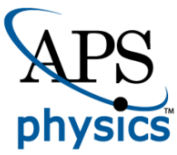

Depolarization Dynamics in a Strongly Interacting Solid-State Spin Ensemble

Joonhee Choi, Soonwon Choi, Georg Kucsko, Peter C. Maurer, Brendan J. Shields, Hitoshi Sumiya, Shinobu Onoda, Junichi Isoya, Eugene Demler, Fedor Jelezko, Norman Y. Yao, and Mikhail D. Lukin

Phys. Rev. Lett. **118**, 093601 — Published 3 March 2017

DOI: 10.1103/PhysRevLett.118.093601

Depolarization dynamics in a strongly interacting solid-state spin ensemble

Joonhee Choi,[1,2,*] Soonwon Choi,[1,*] Georg Kucsko,[1,*] Peter C. Maurer,[3] Brendan J. Shields,[1] Hitoshi Sumiya,[4] Shinobu Onoda,[5] Junichi Isoya,[6] Eugene Demler,[1] Fedor Jelezko,[7] Norman Y. Yao,[8] and Mikhail D. Lukin[1,†]

[1]*Department of Physics, Harvard University, Cambridge, Massachusetts 02138, USA*
[2]*School of Engineering and Applied Sciences, Harvard University, Cambridge, MA 02138, USA*
[3]*Department of Physics, Stanford University, Stanford, California 94305, USA*
[4]*Sumitomo Electric Industries Ltd., Itami, Hyougo, 664-0016, Japan*
[5]*Takasaki Advanced Radiation Research Institute, National Institutes for Quantum and Radiological Science and Technology, 1233 Watanuki, Takasaki, Gunma 370-1292, Japan*
[6]*Research Centre for Knowledge Communities, University of Tsukuba, Tsukuba, Ibaraki 305-8550, Japan*
[7]*Institut für Quantenoptik, Universität Ulm, 89081 Ulm, Germany*
[8]*Department of Physics, University of California Berkeley, Berkeley, California 94720, USA.*

We study the depolarization dynamics of a dense ensemble of dipolar interacting spins, associated with nitrogen-vacancy centers in diamond. We observe anomalously fast, density-dependent, and non-exponential spin relaxation. To explain these observations, we propose a microscopic model where an interplay of long-range interactions, disorder, and dissipation leads to predictions that are in quantitative agreement with both current and prior experimental results. Our results pave the way for controlled many-body experiments with long-lived and strongly interacting ensembles of solid-state spins.

Electronic spins associated with solid-state point defects are promising candidates for the realization of quantum bits and their novel applications [1–5]. In particular, the precise quantum control of *individual* nitrogen-vacancy (NV) centers in diamond has led to advances in both fundamental physics [6–8] and the development of applications ranging from nanoscale sensing to quantum information science [4, 9–14]. This high degree of control naturally suggests the use of strongly interacting, *dense* NV ensembles to explore quantum many-body dynamics. Indeed, recent experiments demonstrate that such a system is a promising testbed to study controlled many-body spin dynamics and novel quantum phases of matter [15, 16].

However, a key challenge in this context is the apparent reduction of the electronic spin lifetime at high defect densities [17, 18]. Such effects were first observed in phosphorus doped silicon over five decades ago [19], where it was suggested that anomalously fast spin relaxation could arise from electronic hopping between nearby impurities. In addition to reduced spin lifetimes, recent experiments in dense NV ensembles have also observed that this relaxation is relatively insensitive to temperature over a wide range [17, 18], implying that the underlying mechanism is qualitatively different from the phonon-induced depolarization of single, isolated NV centers [20].

In this Letter, we characterize the depolarization dynamics of high-density NV ensembles at room temperature. In particular, we perform spin lifetime measurements under different conditions, varying initial state populations, resonant spin densities, and microwave driving strength. To explain the observed features in the spin dynamics, we introduce a spin-fluctuator model, in which a network of short-lived spins (fluctuators) causes depolarization of nearby NV centers via dipolar interactions. Moreover, additional measurements reveal the presence of charge dynamics, providing a potential microscopic origin for such fluctuators.

Our sample is fabricated from a type-Ib HPHT single crystal diamond with an initial nitrogen concentration of ∼100 ppm. The sample is irradiated with high energy electrons at ∼2 MeV to create vacancies. A high concentration of NV centers was achieved via high fluence and *in situ* annealing. The resulting sample contains ∼ 45 ppm of NV centers, corresponding to a typical dipolar interaction strength, $J \sim (2\pi)$ 420 kHz. The high spin density and strong NV-NV interactions are confirmed by independent measurements [15]. To achieve a high degree of spatial control over the optical excitation region, a diamond nanobeam (300 nm × 300 nm × 20 μm) is created via angle-etching and used for all experiments in this work unless otherwise noted.

Each NV center constitutes an effective spin-1 system, which can be optically initialized, manipulated, and read out at ambient conditions [21]. In the absence of an external magnetic field, the spin states $|m_s = \pm 1\rangle$ are separated from the $|m_s = 0\rangle$ state by a crystal field splitting $\Delta_0 = (2\pi)$ 2.87 GHz. Applying a magnetic field further splits the $|m_s = \pm 1\rangle$ states via a Zeeman shift, which is proportional to the projection of the field onto the NV quantization axis (Fig. 1a). Since NVs can be oriented along any of the four crystallographic axes of the diamond lattice, we can spectrally separate four groups of NV centers $\{A, B, C, D\}$ and independently control them via coherent microwave driving (Fig. 1b). By tuning the direction of the magnetic field, we can additionally tune the number of spectrally overlapping groups and hence the effective density of spins.

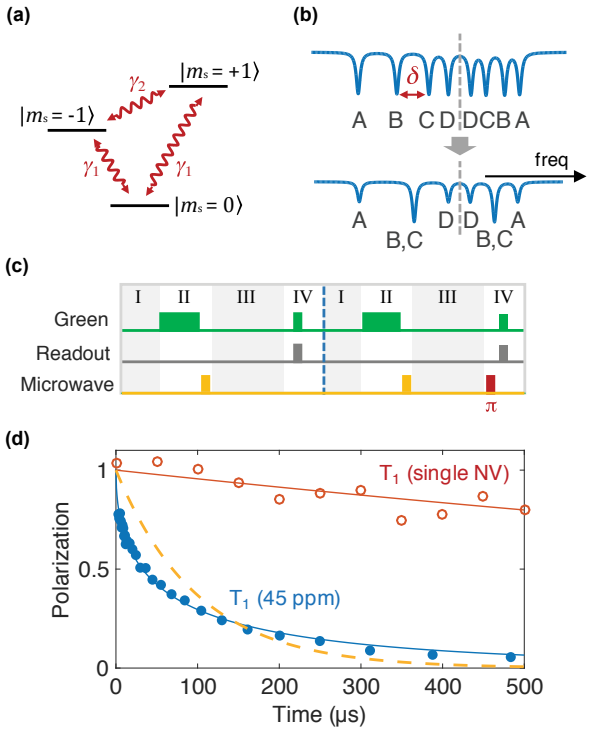

FIG. 1. **Experimental System.** **(a)** Level diagram for NV centers. Red arrows indicate possible spin decay channels, γ_1 and γ_2. **(b)** Schematic electron spin resonance (ESR) spectrum of four subensembles of NV centers A,B,C,D with spectral separation δ between B and C (upper curve). The effective density of resonant spins can be tuned by changing the orientation of the external magnetic field (lower curve). **(c)** Experimental sequence used to measure NV dynamics. I: charge equilibration (∼100 μs duration); II: spin polarization (10 μW laser power, 200 μs duration) and subsequent microwave manipulation to modify the initial state; III: time evolution; IV: spin state readout. Red π-pulse is used to measure the population in an orthogonal state. **(d)** Comparison of depolarization timescales between a single NV (red data, exponential fit) and a dense ensemble of NVs (45 ppm, blue data, stretched-exponential fit with $T_1 \sim 67$ μs). The dashed line is a simple exponential curve with a time constant of 100 μs for comparison.

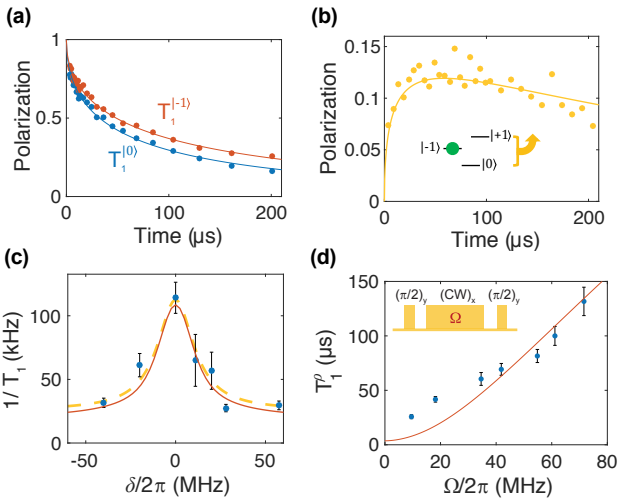

FIG. 2. **Depolarization Dynamics.** **(a)** NV depolarization timescale probed for different initial states. Solid lines represent stretched-exponential fits with corresponding T_1 of 56 ± 2 μs ($|m_s = 0\rangle$, blue data) and 80 ± 2 μs ($|m_s = -1\rangle$, red data). **(b)** Population difference between $|m_s = 0\rangle$ and $|m_s = 1\rangle$ as a function of time for initialization into $|m_s = -1\rangle$. Solid line corresponds to a rate equation model of magnetic noise induced spin depolarization [25]. **(c)** Measured depolarization rates, $1/T_1$, as a function of the spectral distance, δ, between two subensembles B and C. A Lorentzian fit (dashed orange line) is used to extract the full width at half maximum (FWHM) of (2π) 25 ± 6 MHz. **(d)** Spin-lock lifetime T_1^ρ as a function of driving strength Ω. In (c) and (d), red lines indicate the predictions from the spin-fluctuator model at an optimized value of $n_f = 16$ ppm and $\gamma_f = (2\pi)$ 3.3 MHz.

Experiments—To probe the depolarization dynamics of strongly interacting NV ensembles, we utilize the pulse sequence illustrated in Fig. 1c. This sequence allows one to prepare and measure the population in an arbitrary spin state. By repeating a specific sequence with an additional π-pulse (right panel, Fig. 1c), one measures the population of an orthogonal spin state and can use the difference between the two measurements, $P(t)$, to extract the depolarization dynamics [17].

To begin, we measure the depolarization time for a subensemble of NV centers with a particular orientation (Fig. 1d). The observed decay time $T_1 \lesssim 100$ μs is significantly reduced when compared to isolated NVs, where typical lifetimes reach several milliseconds at room temperature [22–24]. Moreover, the decay profile deviates from a simple exponential. Phenomenologically we find that it is characterized by a stretched exponential with exponent 1/2

$$P(t) = e^{-\sqrt{t/T_1}}, \tag{1}$$

consistent with several previous observations [17, 18, 24]. At different spatial locations, the extracted T_1 exhibits small variations possibly due to an inhomogeneous NV concentration.

The depolarization dynamics associated with differing spin states is shown in Fig. 2a,b. For an initial state $|m_s = 0\rangle$, we find a decay time of $T_1 \sim 56$ μs. For an initial state $|m_s = -1\rangle$, however, we observe an extended lifetime, $T_1 \sim 80$ μs, suggesting that the depolarization mechanism is spin-state dependent (Fig. 2a). This is further confirmed by monitoring the population difference between $|m_s = 0\rangle$ and $|m_s = 1\rangle$ after initialization into $|m_s = -1\rangle$ (Fig. 2b). We find that the $|m_s = -1\rangle$ state preferentially decays into the $|m_s = 0\rangle$ state, before reaching a maximally mixed state. Such preferential decay at room temperature is a strong signature that depolarization is induced by an effective magnetic noise [26].

Our next set of measurements probes the density dependence of the NV ensemble's relaxation rate. By tuning the external magnetic field, we can bring two groups of NVs with different orientations of the NV axis into resonance (Fig. 1b). We monitor the depolarization rate of group B, initialized in $|m_s = 0\rangle$, as a function of detuning δ between group B and C. As depicted in Fig. 2c, the depolarization rate increases by a factor of ~ 4 as the two subensembles become degenerate, suggesting that interactions among NV centers play an important role in the depolarization mechanism. Interestingly, the measured width $\Gamma = (2\pi)\ 25 \pm 6$ MHz of this resonant feature significantly exceeds the inhomogeneous linewidth of our sample, $W = (2\pi)\ 9.3 \pm 0.4$ MHz (extracted from an electron spin resonance measurement) as well as the typical dipolar interaction strength [15]. These results imply that the effective magnetic noise originates from interactions among NV centers with a correlation time $\sim 1/\Gamma$.

We further investigate the role of interactions in the depolarization dynamics by performing a spin-locking measurement [27]. The spins are initialized into a superposition state $|+\rangle = (|m_s = 0\rangle + |m_s = -1\rangle)/\sqrt{2}$ and strong microwave driving is then applied along the axis coinciding with this spin state. The driving defines a new dressed-state basis with eigenstates $|+\rangle$ and $|-\rangle = (|m_s = 0\rangle - |m_s = -1\rangle)/\sqrt{2}$, separated in energy by the Rabi frequency of the microwave field, Ω [25]. Following time evolution, the population difference between the $|\pm\rangle$ states is measured.

In the context of NMR, spin-locking is known to decouple nuclear spins from their environment and to suppress dipolar exchange interactions by a factor of two [28, 29]. However, in our case, the combination of spin-locking and the $S = 1$ nature of the NV can cause a *full* suppression of the flip-flop interactions between the $|\pm\rangle$ states at large Ω [15]. We measure the spin-locking relaxation time, T_1^ρ, as a function of Ω as shown in Fig. 2d. At large Ω, we find that T_1^ρ is extended well beyond the bare lifetime T_1.

Spin-Fluctuator Model—One possible mechanism for the fast, density-dependent depolarization observed above is collectively enhanced spontaneous emission (superradiance) [30]. Indeed, in our system, the average NV separation is well below the wavelength of resonant phonons, potentially enabling multiple spins to couple with a single phonon mode. However, the lack of temperature dependence observed in high density samples is inconsistent with a phonon-limited spin lifetime [17]. Another possible explanation is related to spin diffusion induced by dipolar interactions [31]. However, dipolar spin diffusion predominantly affects the boundary of the probed region, and a quantitative estimate suggests a decay which is significantly slower than the observed timescale [25].

To explain our observations, we now introduce a simple phenomenological model, in which we assume that a certain fraction of NV centers undergo rapid incoherent depolarization, providing a mechanism for local energy relaxation [32, 33]. These short-lived spins (termed fluctuators) can then lead to depolarization of the entire ensemble via dipolar interactions (Fig. 3a).

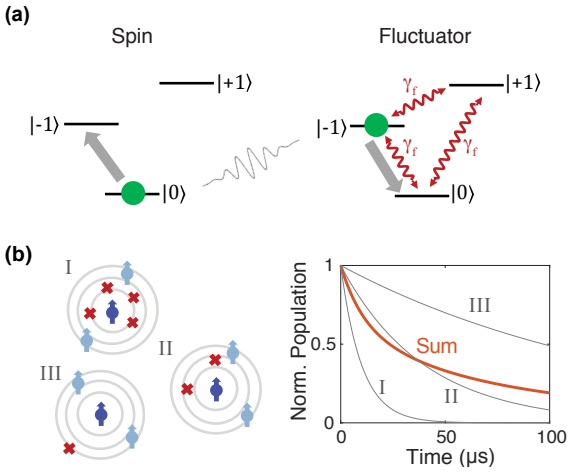

FIG. 3. **Spin-Fluctuator Model. (a)** Level diagram of a single spin and fluctuator in two different spin states (green disk). Red arrows indicate fast depolarization channels of a fluctuator. Solid gray arrows depict spin exchange via dipolar interactions between spin and fluctuator. **(b)** Schematic representation of several spins I, II, and III (dark blue) in the ensemble with different depolarization rates owing to random positions of surrounding fluctuators (red crosses). Ensemble averaging of such depolarization rates gives rise to a stretched exponential (red solid line).

We now focus on the quantitative analysis of ensemble depolarization arising from the interplay of dipolar interactions, disorder, and dissipative fluctuator dynamics. Let us assume that fluctuators are randomly positioned in the lattice at density n_f and depolarize at rate γ_f (Fig. 3a). When γ_f dominates the dipolar interaction strength, each fluctuator can be treated as a localized magnetic noise source with spectral width $2\gamma_f$ (half width at half maximum). From Fermi's Golden rule, the depolarization rate of an NV spin induced by a nearby fluctuator is

$$\gamma_s(\vec{r}) \sim \left(\frac{J_0}{r^3}\right)^2 \frac{2\gamma_f}{(\delta\omega)^2 + (2\gamma_f)^2} \qquad (2)$$

where $\vec{r}$ is distance between the fluctuator and the spin, $J_0 = (2\pi)\ 52$ MHz·nm^3 is the dipolar interaction strength, and $\delta\omega$ is the difference in transition frequencies from the inhomogeneous broadening W [25]. For each spin, the effective depolarization rate is obtained by summing over all fluctuator-induced decay rates: $\gamma_s^{\text{eff}} = \sum_{i\in\text{fluctuators}} \gamma_s(\vec{r}_i)$ (Fig. 3b). Owing to the random position of fluctuators, γ_s^{eff} follows a probability distribution, $\rho(\gamma) = e^{-1/4\gamma T}/\sqrt{4\pi\gamma^3 T}$ with the characteristic

timescale

$$\frac{1}{T} = \left(\frac{4\pi n_f J_0 \bar{\eta}}{3}\right)^2 \frac{\pi}{\gamma_f}, \tag{3}$$

where $\bar{\eta}$ characterizes both the spin exchange matrix element (averaged over all orientations) and the inhomogeneous broadening [25].

This model quantitatively captures all of the observations in our experiments. First, resonant dipolar interactions only allow for the exchange of a single unit of spin angular momentum, naturally explaining the spin-state dependence of the depolarization rate. Second, the stretched exponential profile of $P(t)$ arises from integrating over the distribution $\rho(\gamma_s^{\text{eff}})$; in particular, while each individual spin undergoes a simple exponential decay, the macroscopic ensemble depolarizes with an averaged profile $P(t) = \int_0^\infty \rho(\gamma) e^{-\gamma t} d\gamma = e^{-\sqrt{t/T}}$, precisely matching Eq. (1) (Fig. 3b). We emphasize that the functional form of $\rho(\gamma)$ results from a combination of dimensionality and the long-range power-law [34]; more generally, when the spin-spin interaction scales as $\sim 1/r^\alpha$ in a d-dimensional system, one expects a decay profile, $P(t) = \exp[-(t/T)^{d/2\alpha}]$ [25]. Third, when the two NV groups are tuned into resonance, $\delta = 0$, the effective density of fluctuators n_f doubles, thereby enhancing the depolarization rate by a factor of ~ 4, consistent with our previous observations. By computing the effective NV decay rates ($1/T_1$) as a function of δ and comparing with the experimental data (Fig. 2c), we can extract the density $n_f \sim 16$ ppm and the average decay rate of fluctuators $\gamma_f \sim (2\pi)$ 3.3 MHz [25]. Finally, the extension of the spin lifetime via spin-locking is captured by the suppression of flip-flop interactions [15]. In the ideal case, where the depolarization mechanism results only from resonant exchange, this should lead to a factor of 12 improvement in T_1^ρ as compared to T_1 [25]. However, since T_1^ρ is also affected by interactions with NV spins in non-resonant groups, we expect a more modest enhancement in the experiment. Incorporating both effects, we compare the theory-predicted lifetimes with the experimental data in Fig. 2d, finding reasonable agreement without any additional free parameters.

Charge Dynamics—The extracted fluctuator density, $n_f \sim 16$ ppm, is a sizable fraction of the 45 ppm of NV spins present in our sample. In practice, such fluctuators may arise as a consequence of charge dynamics. More specifically, electrons may tunnel among a network of closely spaced NV centers, and as the charge state of an NV center changes, its spin state is not necessarily conserved. We note that such dynamics inevitably occur in high density spin ensembles when impurity wavefunctions overlap and foreshadow the formation of an impurity band [19].

To probe the existence of such charge hopping, we optically induce a non-equilibrium charge distribution in our bulk diamond sample and monitor the subsequent relaxation back to equilibrium. In the presence of optical illumination at 532 nm, a small fraction of NV centers located at the intensity maximum are excited to the conduction band via a two photon process. Electrons in the conduction band are delocalized and can recombine with neutral nitrogen-vacancy defects (NV^0) located within a mean free path. This charge redistribution can be experimentally measured by scanning a yellow ($\lambda = 594$ nm) probe laser beam, which selectively excites NV^-, relative to the position of the strong ionization beam at $\lambda = 532$ nm (Fig. 4a,b) [6, 35]. Fig. 4c depicts the creation of a non-uniform charge distribution, with electron depletion at the position of the ionization beam and a surplus in the surrounding regions. By monitoring the NV charge state at the origin, after a variable dark interval, we extract a charge recovery timescale of ~ 100 μs as illustrated in Fig. 4d. Interestingly, this recovery occurs in the absence of both optical and thermal excitation, supporting the picture of tunneling-mediated charge diffusion. Such fluorescence dynamics have previously been observed in dilute samples on much slower timescales [36]. Using a classical diffusion equation, we find a timescale for charge hopping T_{hop} ~10 ns, which is comparable to the independently extracted fluctuator decay time $1/\gamma_f$ [25]. This analysis strongly supports the hypothesis that spin

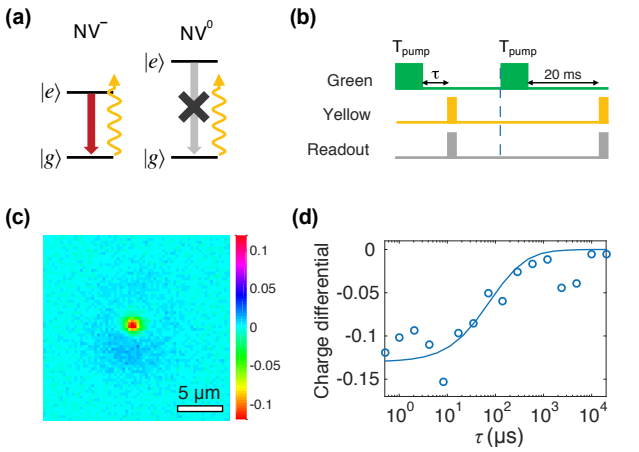

FIG. 4. **Charge-State Dynamics (a)** Level diagram, showing optical ground state, $|g\rangle$, and excited state, $|e\rangle$, for NV^0 and NV^- under illumination. Yellow laser ($\lambda = 594$ nm) can off-resonantly excites NV^-, leading to a strong fluorescence signal. NV^0, however, remains in its ground state due to a higher transition frequency, allowing optical detection of NV charge states. **(b)** Pulse sequence used to measure charge distribution. A green laser is used to create an out-of equilibrium initial state. The resulting charge distribution can be measured via short yellow laser pulses. **(c)** Relative charge distribution measured via a yellow scanning laser (27 μW) after a strong green laser illumination at the center (100 μW). **(d)** Relaxation of charge distribution at the center over time (open circles) and theoretical fit based on a classical diffusion model (solid line).

fluctuators are associated with charge hopping between proximal NV centers.

Conclusion—We have investigated the depolarization dynamics in a dense ensemble of interacting NV centers and have proposed a spin-fluctuator model that quantitatively captures all of the observed dynamics. Moreover, we suggest a possible microscopic understanding for these fluctuators based on tunneling-mediated charge dynamics. We demonstrate that fluctuator-induced depolarization can be mitigated by advanced dynamical decoupling techniques. In particular, the use of spin-locking allows one to explore many-body quantum dynamics at long time scales well beyond bare T_1 [15, 16]. Furthermore, we expect that the depolarization can be controlled by altering the Fermi level via doping [37]. In such highly doped, disordered systems, experiments of the kind reported here could provide new insights into coupled spin and charge dynamics, complementary to conventional transport measurements. We also note that the experimental techniques as well as the theoretical model in the present work can be readily adapted to other types of strongly interacting, solid state spin defects. Thus, our results could provide important guidelines for understanding the nature of many-body dynamics in strongly interacting spin ensembles [38, 39].

We thank N. P. De Leon, V. Oganesyan, A. Gali, D. Budker, A. Sipahigil, M. Knap and S. Gopalakrishnan for insightful discussions and experimental assistance. This work was supported in part by CUA, NSSEFF, ARO MURI, Moore Foundation, Miller Institute for Basic Research in Science, Kwanjeong Educational Foundation, Samsung Fellowship, NSF PHY-1506284, NSF DMR-1308435, Japan Society for the Promotion of Science KAKENHI (No. 26246001), EU (FP7, Horizons 2020, ERC), DFG, Volkswagenstiftung and BMBF.

* These authors contributed equally to this work
† E-mail at:lukin@physics.harvard.edu

[1] L. Childress, R. Walsworth, and M. Lukin, Physics Today **67**, 38 (2014).
[2] F. Dolde, I. Jakobi, B. Naydenov, N. Zhao, S. Pezzagna, C. Trautmann, J. Meijer, P. Neumann, F. Jelezko, and J. Wrachtrup, Nature Physics **9**, 139 (2013).
[3] X. Michalet, F. Pinaud, L. Bentolila, J. Tsay, S. Doose, J. Li, G. Sundaresan, A. Wu, S. Gambhir, and S. Weiss, science **307**, 538 (2005).
[4] I. Lovchinsky, A. Sushkov, E. Urbach, N. de Leon, S. Choi, K. De Greve, R. Evans, R. Gertner, E. Bersin, C. Müller, *et al.*, Science **351**, 836 (2016).
[5] R. Amsüss, C. Koller, T. Nöbauer, S. Putz, S. Rotter, K. Sandner, S. Schneider, M. Schramböck, G. Steinhauser, H. Ritsch, *et al.*, Physical Review Letters **107**, 060502 (2011).
[6] G. Waldherr, P. Neumann, S. Huelga, F. Jelezko, and J. Wrachtrup, Physical Review Letters **107**, 090401 (2011).
[7] W. Pfaff, T. H. Taminiau, L. Robledo, H. Bernien, M. Markham, D. J. Twitchen, and R. Hanson, Nature Physics **9**, 29 (2013).
[8] B. Hensen, H. Bernien, A. Dréau, A. Reiserer, N. Kalb, M. Blok, J. Ruitenberg, R. Vermeulen, R. Schouten, C. Abellán, *et al.*, Nature **526**, 682 (2015).
[9] J. Maze, P. Stanwix, J. Hodges, S. Hong, J. Taylor, P. Cappellaro, L. Jiang, M. G. Dutt, E. Togan, A. Zibrov, *et al.*, Nature **455**, 644 (2008).
[10] G. Kucsko, P. Maurer, N. Y. Yao, M. Kubo, H. Noh, P. Lo, H. Park, and M. D. Lukin, Nature **500**, 54 (2013).
[11] H. Mamin, M. Kim, M. Sherwood, C. Rettner, K. Ohno, D. Awschalom, and D. Rugar, Science **339**, 557 (2013).
[12] P. C. Maurer, G. Kucsko, C. Latta, L. Jiang, N. Y. Yao, S. D. Bennett, F. Pastawski, D. Hunger, N. Chisholm, M. Markham, *et al.*, Science **336**, 1283 (2012).
[13] N. Y. Yao, L. Jiang, A. V. Gorshkov, Z.-X. Gong, A. Zhai, L.-M. Duan, and M. D. Lukin, Physical Review Letters **106**, 040505 (2011).
[14] N. Y. Yao, L. Jiang, A. V. Gorshkov, P. C. Maurer, G. Giedke, J. I. Cirac, and M. D. Lukin, Nature Communications **3**, 800 (2012).
[15] G. Kucsko, S. Choi, J. Choi, P. C. Maurer, H. Sumiya, S. Onoda, J. Isoya, F. Jelezko, E. Demler, N. Y. Yao, and M. D. Lukin, arXiv preprint arXiv:1609.08216 (2016).
[16] S. Choi, J. Choi, R. Landig, G. Kucsko, H. Zhou, J. Isoya, F. Jelezko, S. Onoda, H. Sumiya, V. Khemani, *et al.*, Nature (in press) (2017).
[17] M. Mrózek, D. Rudnicki, P. Kehayias, A. Jarmola, D. Budker, and W. Gawlik, EPJ Quantum Technology **2**, 1 (2015).
[18] A. Jarmola, A. Berzins, J. Smits, K. Smits, J. Prikulis, F. Gahbauer, R. Ferber, D. Erts, M. Auzinsh, and D. Budker, Applied Physics Letters **107**, 242403 (2016).
[19] G. Feher and E. Gere, Physical Review **114**, 1245 (1959).
[20] K. Shrivastava, physica status solidi (b) **117**, 437 (1983).
[21] N. Manson, J. Harrison, and M. Sellars, Physical Review B **74**, 104303 (2006).
[22] D. Redman, S. Brown, R. Sands, and S. Rand, Physical Review Letters **67**, 3420 (1991).
[23] M. Walker, Canadian Journal of Physics **46**, 1347 (1968).
[24] A. Jarmola, V. Acosta, K. Jensen, S. Chemerisov, and D. Budker, Physical Review Letters **108**, 197601 (2012).
[25] See Supplemental Material [url], which includes Ref. [40].
[26] S. Kolkowitz, A. Safira, A. High, R. Devlin, S. Choi, Q. Unterreithmeier, D. Patterson, A. Zibrov, V. Manucharyan, H. Park, *et al.*, Science **347**, 1129 (2015).
[27] S. Hartmann and E. Hahn, Physical Review **128**, 2042 (1962).
[28] N. Bar-Gill, L. M. Pham, A. Jarmola, D. Budker, and R. L. Walsworth, Nature Communications **4**, 1743 (2013).
[29] M. J. Biercuk, H. Uys, A. P. VanDevender, N. Shiga, W. M. Itano, and J. J. Bollinger, Nature **458**, 996 (2009).
[30] R. H. Dicke, Physical Review **93**, 99 (1954).
[31] J. Cardellino, N. Scozzaro, M. Herman, A. J. Berger, C. Zhang, K. C. Fong, C. Jayaprakash, D. V. Pelekhov, and P. C. Hammel, Nature Nanotechnology **9**, 343 (2014).
[32] G. Berman, B. Chernobrod, V. Gorshkov, and V. Tsifrinovich, Physical Review B **71**, 184409 (2005).
[33] B. Vugmeister, Physica Status Solidi (b) **90**, 711 (1978).
[34] L. Levitov, Physical Review Letters **64**, 547 (1990).

[35] B. Shields, Q. Unterreithmeier, N. De Leon, H. Park, and M. Lukin, Physical review letters **114**, 136402 (2015).
[36] K. Iakoubovskii, G. Adriaenssens, and M. Nesladek, Journal of Physics: Condensed Matter **12**, 189 (2000).
[37] Y. Doi, T. Fukui, H. Kato, T. Makino, S. Yamasaki, T. Tashima, H. Morishita, S. Miwa, F. Jelezko, Y. Suzuki, *et al.*, Physical Review B **93**, 081203 (2016).
[38] N. Y. Yao, C. R. Laumann, S. Gopalakrishnan, M. Knap, M. Mueller, E. A. Demler, and M. D. Lukin, Physical Review Letters **113**, 243002 (2014).
[39] M. Serbyn, M. Knap, S. Gopalakrishnan, Z. Papić, N. Y. Yao, C. Laumann, D. Abanin, M. D. Lukin, and E. A. Demler, Physical Review Letters **113**, 147204 (2014).
[40] C. Gardiner and P. Zoller, *Quantum noise: a handbook of Markovian and non-Markovian quantum stochastic methods with applications to quantum optics*, Vol. 56 (Springer Science & Business Media, 2004).